International Journal of Naval Architecture and Ocean Engineering 13 (2021) 57–64

Contents lists available at ScienceDirect

International Journal of Naval Architecture and Ocean Engineering

journal homepage: http://www.journals.elsevier.com/international-journal-of-naval-architecture-and-ocean-engineering/

Representation of small passenger ferry maneuvering motions by practical modular model

Ardhana Wicaksono*, Naoya Hashimoto, Tomoyasu Takahashi

Research and Innovation Center, Furuno Electric Co., Ltd., Hyogo, Japan

ARTICLE INFO

Article history:
Received 12 October 2020
Received in revised form
30 November 2020
Accepted 30 December 2020
Available online 4 February 2021

Keywords:
Maneuvering simulation
MMG model
Simple empirical formulae
Passenger ferry
Sea experiment

ABSTRACT

Maneuvering motions of a ship in calm water are studied through the concept of MMG model. Governing forces are defined by the use of available empirical formulae that require only main ship particulars as input variables. In order to validate the calculation tool, a full-scale sea experiment was carried out in Osaka Bay using a 17-m twin-screw passenger ferry. Test execution and data measurement were performed through the utilization of an autopilot control unit and satellite compass. The result of a straight running test confirms the acceptable accuracy in addressing the surge motion problem. Reasonable agreement between simulation and experiment is also confirmed for 5°/5° and 10°/10° zig-zag tests despite the strong environmental disturbance. The current model can generally represent the subject ship maneuvering motions and is promising for the application to other ship hulls.

1. Introduction

In order to address a ship control problem, reasonable prediction of motions in the horizontal plane is essential. One of prediction methods is the so-called system-based maneuvering simulation model. This approach requires a set of hydrodynamic derivatives and coefficients to express the forces in maneuvering motion. There are various ways to determine these derivatives, such as system identification, free-running model test, captive model tests and virtual model test by the use of Reynolds-averaged Navier-Stokes (RaNS) solver. Among these methods, the captive model test is known to be the most common practice based on questionnaire by ITTC (2017). This indicates high reliability of the captive measurement, especially to capture the nonlinear terms arising in a condition of large drift angle or high yaw rate. However, the need of highly-specialized test environment often limits its applicability.

As optional substitute to the tank experiment, a considerable amount of researches have been done to devise empirical formulae of the maneuvering derivatives. This line of work mostly relies on the regression analysis of experimental data to estimate the relationships between maneuvering derivatives and ship particulars. Inoue et al. (1978) conducted captive measurements on 10 ship models, and accordingly proposed the approximate formulae for linear hull coefficients. With similar concept, Kijima et al. (1990) carried out captive tests on 13 ship models and then introduced the estimation formula for first- and higher-order hull derivatives, as well as the hull-propeller-rudder interaction coefficients. Then, Yoshimura and Masumoto (2011) introduced a set of approximation formulae based on the hydrodynamic database of medium high-speed merchant ships and fishing vessels. Recently, Sukas et al. (2019) presented a summary of published works in this topic and gave general outline of the empirical formulae.

Despite the ease of maneuvering derivatives estimation, the empirical formulae have their own drawbacks. ITTC (2008) reported that the accuracy of most of empirical formulae depends strongly on the experimental data used in the regression; therefore the reliability is fairly limited. It is also common to construct the estimation formulae using the global ship particulars, such as C_B, B, L_{PP} and d, so that the hull form details cannot be accounted. In addition, the benchmark study documented by Stern and Agdrup (2009) using several model ships also indicated that significant scatter was observed in the simulation results obtained by empirical methods. Even though several empirical formulae gave relatively good accuracy, the remaining formulae gave large scatter due to the limitation of their range-of-applicability. Then, the Research Committee on Improvement of Mathematical Model for Ship

* Corresponding author.
E-mail address: wicaksono.ardhana.nt@furuno.co.jp (A. Wicaksono).
Peer review under responsibility of The Society of Naval Architects of Korea.

https://doi.org/10.1016/j.ijnaoe.2020.12.006

Nomenclature

$\prime$	Symbol for nondimensional quantity
U	Resultant velocity ($=\sqrt{u^2+v^2}$) [m/s]
ψ, β	Heading angle, drift angle [rad]
u, v, r	Velocity (or rate) of surge, sway and yaw [m/s, rad/s]
m, I_{zz}	Ship mass and moment of inertia [kg, kg m^2]
m_x, m_y, J_z	Added masses in longitudinal and lateral directions, added moment of inertia [kg, kg m^2]
k'_{zz}	Nondimensional yaw gyrational radius [-]
$\dot{u}$, $\dot{v}$, $\dot{r}$	Acceleration of surge, sway and yaw [m/ s^2, rad/ s^2]
δ, $\dot{\delta}$	Rudder angle, rudder turning rate [rad, rad/ s]
n_P, n_E	Propeller rotational speed, engine rotational speed [rad/s]
GM	Metacentric height [m]
X_H, Y_H, N_H	Hull-induced surge force, sway force, yaw moment [N, N m]
X_R, Y_R, N_R	Rudder-induced surge force, sway force, yaw moment [N, N m]
X_P	Propeller-induced surge force [N]
ρ	Water density [kg/m^3]
L_{PP}, L_{OA}	Length between perpendiculars, Length overall [m]
B	Ship breadth [m]
C_B	Block coefficient [-]
d	Ship draft [m]
R_0	Calm water resistance [N]
Y'_v, Y'_r, N'_v, N'_r	First-order (linear) hull derivatives with respect to sway velocity and yaw rate [-]
X'_{vv}, X'_{rr}, X'_{vr}, X'_{vvvv}, Y'_{vvv}, Y'_{vvr}, Y'_{vrr}, Y'_{rrr}, N'_{vvv}, N'_{vvr}, N'_{vrr}, N'_{rrr}	High-order (nonlinear) hull derivatives with respect to sway velocity and yaw rate [-]
t_P	Thrust deduction coefficient [-]
T	Propeller thrust [N]
D_P	Propeller diameter [m]
P/D, A_E/A_O, n	Propeller pitch ratio, expanded area ratio, number of blade [-]
K_T	Thrust coefficient [-]
J_P	Propeller advance ratio [-]
k_0, k_1, k_2	Propeller open-water polynomials [-]
w_P	Propeller wake fraction [-]
t_R	Coefficient of rudder resistance deduction [-]
F_N	Rudder normal force [N]
H	Water depth [m]
a_H	Coefficient of rudder force increase [-]
x_R	Longitudinal position of rudder [m]
x_H	Longitudinal position of additional lateral force acting point [m]
A_R	Representative rudder area [m^2]
U_R	Resultant velocity into rudder [m/s]
f_α	Rudder lift force coefficient [-]
α_R	Effective rudder inflow angle [rad]
u_R, v_R	Longitudinal and lateral components of rudder inflow velocity [m/s]
ε	Ratio between rudder wake fraction and propeller wake fraction ($=(1-w_R)/(1-w_p)$) [-]
η	Ratio between propeller diameter and rudder height ($=D_P/H_R$) [-]
κ	Experimental coefficient related to u_R [-]
γ_R	Flow straightening coefficient [-]
B_R, H_R	Rudder breadth (chord), rudder height (span) [m]
H_m, T_m	Mean wave height, mean wave period [m, s]
U_W, U_C	Wind velocity, current velocity [m/s]
t	Time [s]

Maneuvering Predictions (2014) inside the Japan Society of Naval Architects and Ocean Engineers (JASNAOE) performed an investigative study to check the ship parameters that govern the change of linear maneuvering derivatives. In their analysis, they used the data of 23 ship models' captive tests conducted in Kyushu University, Hiroshima University and Hokkaido University. The committee found that the correlation between the ship dimensions and maneuvering derivatives shown by the coefficient of determination (R^2) changed significantly depending on the data selection used in the fitting. For example, the large change of R^2 was found when taking account the data from Hokkaido University that includes some vessels which have distinct frame lines. In case of the analysis using all data from 23 ship models, they found that only the fitting of N'_v and $2d/L$ which shows strong correlation ($R^2 > 0.5$). They finally concluded that the quality and consistency of captive tests data is vital to construct an empirical method. Hence, it is acknowledged that the empirical formulae might not give highly accurate result when compared to the sea trial or free-running test; however it may serve as a great insight at preliminary design stage.

Therefore, our study is aimed to present a suitable mix of available empirical relations which can be used as a practical calculation tool of ship maneuvering motion. Modular-type mathematical model based on MMG approach is employed to describe the forces induced by hull, propeller and rudder, as well as their interactions. Finally, in order to validate our calculation results, a full-scale sea-experiment is performed using a passenger ferry; and the comparability between computation results and measured data is discussed.

2. MMG model and its essential features

More than half century ago, the maneuvering motions of a ship were simply defined through a "Response Model" expressed by the relation between δ and r. The ship hull characteristics are consolidated into two constants: K and T. Despite the strong simplification, this model is known to be practical in the evaluation of course-keeping ability. This approach was introduced by Nomoto et al. (1956) and is still being used nowadays.

Since this K-T model does not solve the complete motion equation, there is no exact mean to understand the ship acceleration, velocity and its position, which are essential to tackle a ship control problem. Due to this reason, a research group called Mathematical Modeling Group of Maneuvering Motion, abbreviated as MMG, was established in Japan. The mission was to develop and introduce a "Hydrodynamic Model" with proper motion equations, along with detailed force expressions and the required experimental procedure (Ogawa et al., 1977). Then recently, the Research Committee on Standardization of Mathematical Model for Ship Maneuvering Predictions (2012) of JASNAOE conducted a study on the general adaptability and applicability of MMG model. Accordingly, Yasukawa and Yoshimura (2015) proposed the "MMG standard method" and introduced its essential characteristics. In this research, the numerical model will mostly follow the MMG

standard method, while practical approaches are adopted to determine hydrodynamic derivatives and coefficients.

2.1. Theoretical assumptions

MMG standard method requires some assumptions to be satisfied prior to the simulation. Those are (a) ship as a rigid body; (b) quasi-steady assumption; (c) low v compared to u; (d) adequately low u to assure negligibly-small steady wave making; (e) considerably large value of GM resulting negligible roll coupling; (f) δ and n_P are considered given. It is noteworthy that these features are commonly suitable for large merchant ships in oceangoing operation.

2.2. Equations of motions

The hydrodynamic problem is simplified so that the ship motions in concern are only those in horizontal plane. Fig. 1 presents two different coordinate systems: the body-fixed $O-xy$ system and the space-fixed $O-x_0y_0$ system, originating from the ship's center of gravity O. The vertically-extending z-axis is independent from them.

By expressing the maneuvering forces and moment by Newton's Law and performing the coordinate systems transformation, we may formulate our equations of motions in the surge-sway-yaw coupled form as

$$\begin{aligned}(m+m_x)\dot{u}-(m+m_y)vr &= X_H+X_R+X_P,\\ (m+m_y)\dot{v}+(m+m_x)ur &= Y_H+Y_R,\\ (I_{zz}+J_z)\dot{r} &= N_H+N_R,\end{aligned} \tag{1}$$

with the subscripts H, R and P on the right-hand side signify the force contributions from hull, rudder and propeller, respectively. Ship mass, added masses and added moment of inertia have also been included.

Therefore, once these terms can be estimated, the three acceleration unknowns ($\dot{u}$, $\dot{v}$, $\dot{r}$) can be readily obtained. Subsequently, the ship velocities and positions in space may be computed by appropriate time-stepping scheme, such as Euler or Runge-Kutta method. Therefore, it is understood that the accurate estimation of forcing functions plays a vital role in representing ship behavior under maneuvering motions.

2.3. Hull forces

Under zero encounter-frequency assumption, Yasukawa and Yoshimura Yasukawa and Yoshimura (2015) defined X_H, Y_H and N_H as

$$\begin{aligned}X_H &= \left(\frac{1}{2}\right)\rho L_{PP}dU^2X'_H(v',r'),\\ Y_H &= \left(\frac{1}{2}\right)\rho L_{PP}dU^2Y'_H(v',r'),\\ N_H &= \left(\frac{1}{2}\right)\rho L_{PP}^2dU^2N'_H(v',r').\end{aligned} \tag{2}$$

X'_H, Y'_H and N'_H are expressed as polynomial functions of $v'(=v/U)$ and $r'(=rL_{PP}/U)$:

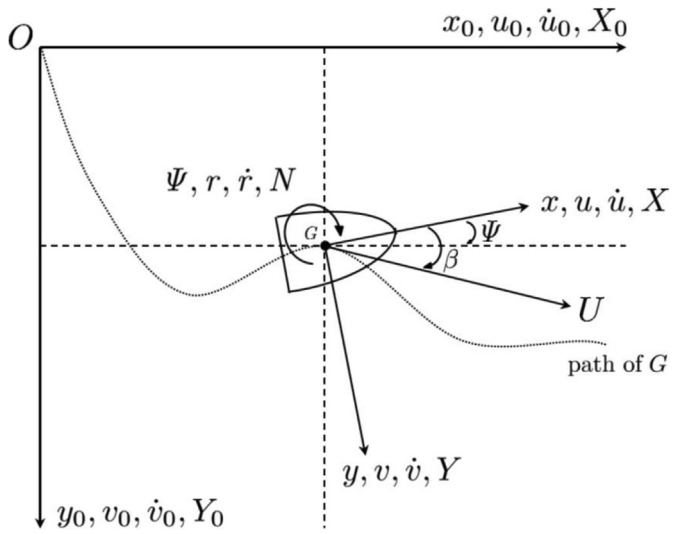

Fig. 1. Coordinate systems of ship maneuvering motions.

$$\begin{aligned}X'_H(v',r') &= -R'_0+X'_{vv}v'^2+X'_{vr}v'r'+X'_{rr}r'^2+X'_{vvvv}v'^4,\\ Y'_H(v',r') &= Y'_vv'+Y'_rr'+Y'_{vvv}v'^3+Y'_{vvr}v'^2r'+Y'_{vrr}v'r'^2+Y'_{rrr}r'^3,\\ N'_H(v',r') &= N'_vv'+N'_rr'+N'_{vvv}v'^3+N'_{vvr}v'^2r'+N'_{vrr}v'r'^2+N'_{rrr}r'^3,\end{aligned} \tag{3}$$

Hence, it is confirmed that we require 1 surge resistance coefficient and 16 maneuvering derivatives in order to solve Eq. (2).

2.4. Propeller force

Acting as the main ship propulsor, the surge force generated by a propeller is defined as

$$X_P=(1-t_P)T, \tag{4}$$

$$T=\rho n_P^2D_P^4K_T. \tag{5}$$

Here, the induced lateral force and yawing moment are assumed to be negligible due to the coupled operation of the twin propeller under the same n_p. Then, K_T is commonly expressed as the polynomial function of J_P as

$$K_T(J_P)=k_2J_P^2+k_1J_P+k_0, \tag{6}$$

$$J_P=\frac{u(1-w_P)}{n_PD_P}. \tag{7}$$

Hence, there are at least 5 parameters (t_p, k_0, k_1, k_2, w_P) to be estimated in order to solve Eq. (4). It is noteworthy that a constant value of w_P in the straight running condition, as well as t_P, are used in the simulations following the approach of Yoshimura and Masumoto (2011). This assumption comes from the observation that the $(1-w_P)$, as well as the u_R, have the tendency to be relatively constant even in large v and r. Similar observations are also reported in Yoshimura and Nagashima (1985) and Lee et al. (1988).

2.5. Rudder forces

The fluid forces due to the rudder action can be expressed as:

$$\begin{aligned} X_R &= -(1-t_R)F_N \sin\delta, \\ Y_R &= -(1+a_H)F_N \cos\delta, \\ N_R &= -(x_R + a_H x_H)F_N \cos\delta, \end{aligned} \tag{8}$$

with the rudder normal force being explained as

$$F_N = \left(\frac{1}{2}\right)\rho A_R U_R^2 f_\alpha \sin\alpha_R. \tag{9}$$

In order to determine the U_R ($=\sqrt{u_R^2+v_R^2}$), we should start by approximating u_R and v_R. In the MMG standard method, the x-component is defined as

$$u_R = \varepsilon(1-w_P)u\sqrt{\eta\left\{1+\kappa\left(\sqrt{1+8K_T/\pi J_P^2}-1\right)\right\}^2 + 1 - \eta}, \tag{10}$$

which is suitable only for the first quadrant of ship speed and propeller operation ($u > 0$, $n_P > 0$). Then, by taking the definition of effective rudder inflow angle α_R as

$$\alpha_R = \delta + \frac{v_R}{u_R} \simeq \delta + \frac{\gamma_R\{-(v+x_R r)\}}{u_R}, \tag{11}$$

we realize that the y-component can be approximated as

$$v_R = \gamma_R\{-(v+x_R r)\}. \tag{12}$$

Accordingly, we identified at least 6 constants (t_R, a_H, x_H, ε, κ, γ_R) to be determined in order to solve Eq. (8).

3. Test ship and measurement apparatus

Subject ship used in the experiment was newly-introduced to the experimental fleet of the authors' institution. Her name is Furuno Maru, a passenger ferry equipped with twin screw system (see Fig. 2). Principal particulars and other necessary input data to the simulator are listed in Table 1. These particulars have been defined based on the assumptions that: 1) the ship is to be treated as displacement-type hull, despite of planing behavior at top speed; 2) the average draft is taken due to the small trim (0.5 m aft draft against 0.46 m fore draft), and even-keel condition is presumed.

In order to support many kinds of sea experiments, Furuno Maru is equipped with various sensors and devices. Among these instruments, we especially utilized following products:

- Satellite Compass SC-30: measurement of real-time position, heading, ship speed, etc.
- Autopilot Control Unit Navpilot-711: execution of zig-zag test, heading control, etc.

4. Practical estimation methods of forces and moments

In order to achieve reasonable accuracy, the estimation methods of forces induced by the ship hull, propeller and rudder action have to be selected with care. We implied several concepts in the selection of empirical approaches, in which they are preferred to:

- Require input data that are commonly available ship particulars;
- Be of explicit expression that may be computed by the use of simple calculator;
- Be constructed with sensible engineering assumption;

Fig. 2. Subject ship for sea experiment (Furuno Electric Co., Ltd., 2020).

- Be applicable to diverse hull types and have been validated through previous studies.

Through these characteristics, we hope that our numerical scheme may be useful not only for researchers, but more importantly for those in need of practical approach of ship maneuvering prediction.

Our literature survey led us to the selected empirical formulae shown in Table 2. The technical considerations on some of the selections are explained as follows:

- Calm water resistance coefficient strongly depends on the underwater hull shape and the appendages (rudder, shaft, shaft bracket, etc.). In regard to the twin screw system and general hull shape, the ship model in the high-speed maneuverability test of Yasukawa et al. (2014) is considered to be relatively comparable to Furuno Maru. Therefore the constant value of R'_0 is taken from this study as first estimate.
- Hull derivatives and some coefficients are estimated by the formulae of Yoshimura and Masumoto (2011) which are expressed as follows:

$$\begin{aligned} X'_{vv} &= 1.15(C_B B/L) - 0.18, \\ X'_{vr} &= m'_y + 1.91(C_B B/L) - 0.08, \\ X'_{rr} &= -0.085(C_B B/L) + 0.008 - x'_G m'_y, \\ X'_{vvv} &= -6.68(C_B B/L) + 1.10, \end{aligned} \tag{13}$$

Table 1
Principal particulars of Furuno Maru.

Item	Value	Unit
L_{OA}	17.9	m
L_{PP}	14.94	m
B	4.08	m
d	0.48	m
C_B	0.3	(−)
B_R	0.4025	m
H_R	0.805	m
D_P	0.74	m
P/D	1.13	(−)
A_E/A_O	0.75	(−)
n	5	(−)
n_E/n_P	2.57	(−)
$\dot{\delta}$	6.7	°/s

$$
\begin{aligned}
Y'_v &= -(0.5\pi k + 1.4(C_B B/L)),\\
Y'_r &= m'_x + 0.5(C_B B/L),\\
Y'_{vvv} &= -(0.185L/B + 0.48),\\
Y'_{vvr} &= -0.75,\\
Y'_{vrr} &= -(0.26(1-C_B)L/B + 0.11),\\
Y'_{rrr} &= -0.051,
\end{aligned}
\tag{14}
$$

$$
\begin{aligned}
N'_v &= -k,\\
N'_r &= -0.54k + k^2,\\
N'_{vvv} &= 0.69C_B - 0.66,\\
N'_{vvr} &= 1.55(C_B B/L) - 0.76,\\
N'_{vrr} &= -(0.075(1-C_B)L/B - 0.098),\\
N'_{rrr} &= 0.25(C_B B/L) - 0.056,
\end{aligned}
\tag{15}
$$

$$
\begin{aligned}
1 - t_R &= 0.61\\
a_H &= 3.6(C_B B/L)\\
x'_H &= -0.4\\
\varepsilon &= 2.26 - 1.82(1-w_p)\\
\kappa &= 0.55/\varepsilon\\
\gamma_R &= 2.06(C_B B/L) + 0.14
\end{aligned}
\tag{16}
$$

The applicable dimensions of these formulae are as follows: $2.6 < L/B < 7.1$, $0.25 < d/B < 0.46$, $0.51 < C_B < 0.65$, in which the d/B and C_B of Furuno Maru do not satisfy these conditions. However, their formulae were constructed from a database of medium high-speed ships with relatively low values of C_B. For that reason, this database is expected to be more suitable for Furuno Maru and selected speeds in the sea experiment compared to the typical estimation formulae made for full hull merchant ships.

- Considering the circular shape of Furuno Maru's propeller blade, K_T on Eq. (6) is approximated through the polynomial formulation of

$$K_T = \sum_{s,t,u,v} C^T_{s,t,u,v} (J)^s (P/D)^t (A_E/A_0)^u (n)^v \,, \tag{17}$$

where the coefficients $C^T_{s,t,u,v}$ and terms s, t, u, v can be found in Oosterveld and Van Oosanen (1975). The derived expression is obtained through multiple regression analysis on the open-water tests data of 120 B-series propeller models. The applicable range of this formula is as follows: $2 \le n \le 7$, $0.3 \le A_E/A_O \le 1.05$, $0.5 \le P/D \le 1.4$. Referring to the propeller data in Table 1, it is clear that this formula is suitable for the Furuno Maru. In addition, the effect of shaft inclination angle ($= 8^\circ$) to the thrust is considered small, therefore not accounted in the calculation. This tendency has been confirmed by comprehensive experimental works of Taniguchi et al. (1967) and Chattopadhyay et al. (1986).

- Twin screw system is taken into account by equivalent single-rudder model of Okuda et al. (2019). The concept is to replace the twin-propeller twin-rudder system into a single propeller and rudder system mounted on the center line of the ship. Therefore, in case of equal n_p for the twin propeller, the X_P on Eq. (4) and the F_N on Eq. (9) can be transformed respectively into

$$X_P = (1 - t_P)(T_1 + T_2), \tag{18}$$

$$F_N = 2 \times \left(\frac{1}{2}\right) \rho A_R U_R^2 f_\alpha \sin \alpha_R. \tag{19}$$

Finally, the maneuvering coefficients estimated by above approaches are listed in Table 3. It is noteworthy that the ship particulars may not entirely satisfy the range-of-applicability of some estimation formulae. However, we intend to keep a high level of practicality, while understanding the limitation of published experimental data.

Table 2
Estimation methods used in MMG standard method of Yasukawa and Yoshimura (2015) and in this study.

Item	Estimation method	
	MMG standard	Current
m'_x, m'_y, J'_z, k'_{zz}	Motora (1959,1960a,b)	Motora (1959,1960a,b)
R'_0	Oblique towing test	Yasukawa et al. (2014)
X'_{vv}, X'_{vr}, X'_{rr}, X'_{vvvv}, Y'_v, Y'_r, Y'_{vvv}, Y'_{vvr}, Y'_{vrr}, Y'_{rrr}, N'_v, N'_r, N'_{vvv}, N'_{vvr}, N'_{vrr}, N'_{rrr}	Oblique towing test	Yoshimura and Masumoto (2011)
t_P, w_P	Free-running test	Harvald (1983)
k_0, k_1, k_2	Open-water test	Oosterveld and Van Oossanen (1975)
t_R, a_H, x_H, ε, κ, γ_R	Rudder force test	Yoshimura and Masumoto (2011)
Twin screw system		Okuda et al. (2019)

5. Plan of sea experiment

The test site, as enclosed by the broken white line in Fig. 3, is the Osaka Bay area situated south of Nishinomiya City and northwest of Osaka Port. This sea area is sheltered from the open sea by detached fixed breakwater indicated by red solid line. The measured water depth in the site is 11 m in average that gives us the H/d ratio of 22.9, which can be considered as a deep water area for our test ship.

The experiment was done in two days: 27th and January 29, 2020. At first, we did the initial setting of experimental apparatus, including the data retrieval system from the installed sensors. Several tests were also conducted on the operation of autopilot system for zig-zag test. In the remaining time of the first day, we performed seven cases of straight running test.

On the second day, the straight running test was re-executed with the proper step of engine rotational speed. For each case, we did two tests for both head and following sea conditions. Then, we proceeded to $5^\circ/5^\circ$ and $10^\circ/10^\circ$ zig-zag tests with approach speed of 13.4 ($\approx$13) knots and 9.9 ($\approx$10) knots, respectively. It is important to note that the ship enters semi-displacement state and starts to plane when the speed exceeds 16 knots. This planing state is certainly undesirable when considering basic assumptions of MMG model. Therefore, the ship speeds in the experiment were selected based on this physical background and also due to safety consideration.

Prior to each test execution, initially straight approach must be reached before applying a specified amount of rudder angle. Relative to the main wind direction, the approach heading angle was adjusted to the approximate head wind condition (0°). The handling of ship to reach this initial condition (ship speed and relative heading angle to the wind) was executed manually by the ship captain. The summary of cases in this sea experiment is shown in Table 4.

The environmental conditions on the experiment days are summarized as shown in Table 5. The data correspond to the values measured exactly at the starting time of the experiment on both days, which are 13:00 of January 27th and 14:00 of January 29th.

Table 3
Maneuvering derivatives and related coefficients used in simulation.

Item	Value	Item	Value
m'_x	0.007	N'_v	−0.064
m'_y	0.151	N'_r	−0.030
J'_z	0.005	N'_{vvv}	−0.453
R'_0	0.029	N'_{vvr}	−0.591
X'_{vv}	−0.085	N'_{vrr}	−0.094
X'_{vr},	0.227	N'_{rrr}	−0.035
X'_{rr},	−0.001	t_P	0.24
X'_{vvvv},	0.552	w_P	0.2
Y'_v,	−0.215	t_R	0.39
Y'_r,	0.048	a_H	0.29
Y'_{vvv}	−1.157	x_H	−0.4
Y'_{vvr}	−0.75	ε	0.69
Y'_{vrr}	−0.776	κ	0.79
Y'_{rrr}	−0.051	γ_R	0.31

Since the exact wave, wind and current data on the test site could not be obtained; references are taken from following sources:

- Wave record of H_m, T_m and main direction are taken from the observation data in Kobe Port (approximately 8 km west from the test site) published by Japanese Ministry of Land, Infrastructure, Transport and Tourism (2020) through NOWPHAS system.
- Wind velocity and main direction are taken from the observation of Japan Meteorological Agency (2020) at the Kobe Airport (approximately 10 km southwest from the test site).
- Current velocity and main direction are taken from the estimation of Hydrographic and Oceanographic Department of Japan Coast Guard (2020) for Kobe Port Area.

6. Results and discussion

6.1. Note on the simulation and data processing

In order to keep the simplicity of the approach, we prevent ourselves from introducing any environmental disturbance to our model. Calm water condition is assumed, and the influence from environmental loads will be reserved to qualitative discussion for the time being. Moreover, all angular measures (δ, r, ψ, etc.) are processed in the simulations using the SI unit of radian (rad), while the results are shown in degree (°) for the sake of familiar presentation. In addition, the recorded data in the sea experiment were filtered by low-pass Butterworth zero-phase filter with cut-off frequency of 0.5 Hz. Aside of this filter, there is no artificial tuning whatsoever applied to both experimental and calculated data in order to fit to each other.

Fig. 3. Site of the sea experiment (Google Maps, 2020).

6.2. Straight running test

Straight running test can be simulated by imposing certain value of n_P with $\delta \approx 0°$. Therefore, the MMG equations of motions reduce into simple surge motion equation of

$$(m + m_x)\dot{u} = -R_0 + (1 - t_P)T, \tag{20}$$

that leaves only the R_0 and T as the governing terms. Since constant R'_0 is a fixed value, we understand that the remaining user-defined variable in this equation is n_P that accordingly produces thrust. With this concept, we conducted the speed trial. First, the captain controls the lever to reach target n_E (or n_P), and we subsequently record the ship speed ($u \approx U$) once it reaches steady condition. This test was performed with different values of n_P in order to obtain the relation between propeller rotational speed and steady ship speed.

The comparison between simulated results and experimental data is shown in Fig. 4. In overall, it is observed that the simulator can represent the straight-running motion with enough accuracy. Our significant findings are as follows:

- In low speed (<8 knots), the agreement between simulation and experiment is found to be better than those in high-speed region.
- When the ship speed exceeds 16 knots, the ship starts to plane which decreases the total resistance therefore gives rise to the ship speed. At this point onward, the trend changes so that the simulation results underestimated the recorded speeds at experiment.

6.3. Zig-zag test

The purpose of this test is to determine the vessel's yaw-checking and course-keeping abilities. For each case, we measured the U, δ, r and ψ, which are the required quantities to validate our simulator. Figs. 5 and 6 show the time-series of δ, ψ and r obtained from the simulation and experiment of 5°/5° and 10°/10° zig-zag tests, respectively. In addition, Fig. 7 also depictures the time-series of ship speeds from simulation and experiment.

In 5°/5° maneuver, we can see that the environmental disturbance is strongly reflected on the measured data as the fluctuation of r. For instance at the second turning to starboard ($t = 10 \sim 16$ s), the measured steady condition of $\delta = +5°$ was prolonged compared to the calculation due to the decrement of r. In this maneuver as well, the ship heading angle reached its maximum deviations on approximately ±8° relative to the main wind direction. Therefore, there is a high probability that the ship encountered approximate head wind all the time which led to a prominent speed reduction as shown in Fig. 7.

In 10°/10° maneuver, the agreement between the calculation and measured data is remarkable. As defined in the Eq. (8), the N_R is

Table 4
Test cases in sea experiment.

Test	Initial condition	Rudder angle
Straight running	$n_P = 3.89 \sim 12.32$ rad/s	≈0°
Zig-zag	$U_0 = 13.4$ knots (Fn 0.57)	5°/5°
Zig-zag	$U_0 = 9.9$ knots (Fn 0.42)	10°/10°

Table 5
Environmental conditions in sea experiment.

Day	Wave		Wind		Current	
	H_m, T_m	Direction (°)	U_W (m/s)	Direction	U_C	Direction
January 27th, 2020	0.39, 2.8	82	14.3	NE	0–0.2	SE
January 29th, 2020	0.38, 2.9	192	9.4	WSW	0	–

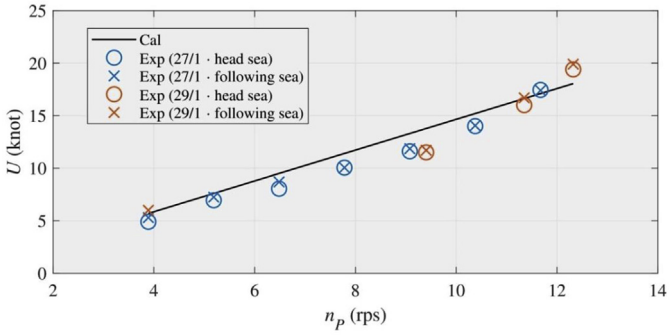

Fig. 4. Relationship between n_P and U in straight running test.

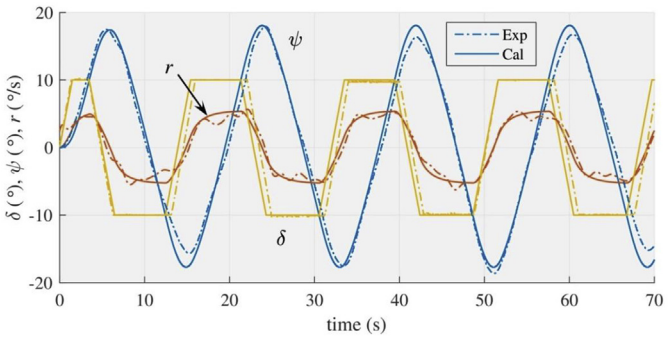

Fig. 6. Time-series of δ, ψ and r in $10^\circ/10^\circ$ zig-zag maneuver.

obviously larger than that in $5^\circ/5^\circ$ case. Hence, the ratio between disturbance-induced yaw rate and rudder-induced yaw rate was naturally reduced so that the time lag between simulation and experiment was suppressed. In addition, the change of ship speed can be accurately estimated. Looking at the fluctuation of U especially at $t > 30$s, we can observe that the peaks correspond to the $\beta \approx 0$ conditions, while the troughs correspond to the conditions of β at maximum.

In overall, the peak values of ψ and r from simulation and experiment are in acceptable agreement for all cases. In this regard, we may imply that the current practical calculation method is able to reproduce the real maneuvering motions of the subject ship to a reasonable degree of accuracy. Nevertheless, we expect the agreement to be improved should the weather condition be milder.

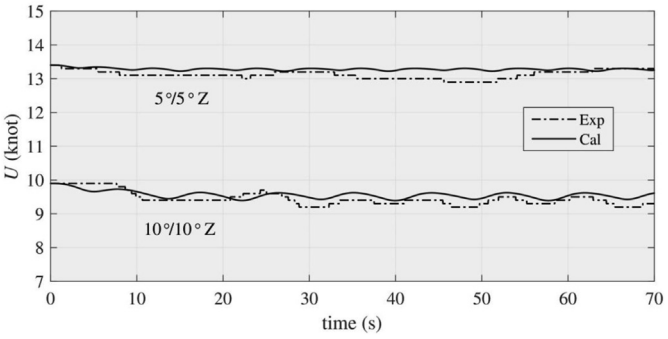

Fig. 7. Time series of U in $5^\circ/5^\circ$ and $10^\circ/10^\circ$ zig-zag maneuvers.

7. Conclusions

Representation of a small passenger ferry maneuvering motions has been made through the utilization of the modular-based MMG model. Practical empirical formulae that require only the general ship particulars have been selected to define the governing forces and moment. In order to validate the computation method, we carried out a full-scale sea experiment using a 17-m passenger ferry in Osaka Bay. Straight running and zig-zag tests were executed, where the initial approach conditions were reached through the captain's manual steering.

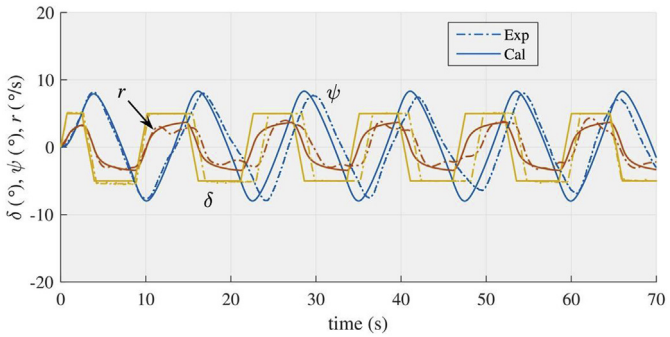

Fig. 5. Time-series of δ, ψ and r in $5^\circ/5^\circ$ zig-zag maneuver.

Through the comparison between calculation and experiment, we observed that the general characteristics of maneuvering motions can be reproduced with reasonable accuracy. Despite of overall agreement, a change on $n_P - U$ relation in the straight running test can be noticed at $U > 16$ knots due to the planing behavior. In case of zig-zag motions, the current model was able to estimate the measured steady values of r and maximum values of ψ in all zig-zag maneuvers. Owing to the calm water assumption, discrepancy between computation and measurement can be recognized due to the strong environmental disturbance (mainly wind and wave). The extensions of current study will be done in order to incorporate the environmental disturbance to the model, as well as the development of dedicated practical maneuvering model for small high-speed craft.

Declaration of competing interest

The authors declare that they have no known competing financial interests or personal relationships that could have appeared to influence the work reported in this paper.

Acknowledgements

The authors would like to extend the gratitude to the Director

and Divisional General Manager of Research and Innovation Center, Dr. Yasushi Nishimori, and General Manager of Research Department, Dr. Tsutomu Okada, for their approval to disclose the experimental data. Appreciation is also reserved to Hiroshi Fukuzaki, the captain of Furuno Maru, for his cooperation so that the experiment could be performed well in relatively rough weather.

References

Chattopadhyay, S., Kato, H., Yamaguchi, H., 1986. A study on performance and cavitation of propellers for high speed crafts including effect of boss. J. Soc. Nav. Archit. Jpn. 159, 59–70. https://www.jstage.jst.go.jp/article/jjasnaoe1968/1986/159/1986_159_59/_article.

Furuno Electric Co, Ltd, 2020. Introduction of a New Experimental Ship "Furuno Maru". Furuno Corporate Information Site. General News. https://www.furuno.co.jp/news/general/general_category.html?itemid=860&dispmid=1017. (Accessed 10 July 2020).

Google Maps, 2020. Osaka Bay 34deg41'40.0"N 135deg20'10.3"E. 2D Map. https://www.google.com/maps/@34.6736597,135.3233158,11240m. Accessed: 10 July 2020.

Harvald, S.A., 1983. Resistance and Propulsion of Ships. Wiley.

Inoue, S., Hirano, M., Hirakawa, Y., Mukai, K., 1978. The hydrodynamic derivatives on ship maneuverability in even keel condition. Trans. West-Jpn. Soc. Naval Archit. 57, 13–19 (in Japanese). https://www.jstage.jst.go.jp/article/wjsna/57/0/57_13/_article/-char/ja.

Ittc, 2008. The maneuvering committee - final report and recommendations to the 25th ITTC. In: Proceedings of the 25th ITTC, vol. 1. Fukuoka.

Ittc, 2017. The maneuvering committee - final report and recommendations to the 28th ITTC. In: Proceedings of the 28th ITTC, vol. 1. Wuxi.

Japan Coast Guard, 2020. Estimated Current Data of January 2020 on Seto Inland Sea. https://www1.kaiho.mlit.go.jp/KANKYO/TIDE/curr_pred/index.htm. Accessed : 20 Novermber 2020.

Japan Meteorological Agency, 2020. Daily Weather Data of January 2020 on Kobe Airport. https://www.data.jma.go.jp/obd/stats/etrn/view/daily_a1.php?prec_no=63&block_no=1587&year=2020&month=01&day=27&view=p1. Accessed: 22 June 2020.

Kijima, K., Katsuno, T., Nakiri, Y., Furukawa, Y., 1990. On the maneuvering performance of a ship with the parameter of loading condition. J. Soc. Nav. Archit. Jpn. 168, 141–148. https://www.jstage.jst.go.jp/article/jjasnaoe1968/1990/168/1990_168_141/_article.

Lee, S.K., Fujino, M., Fukasawa, T., 1988. A study on the manoeuvring mathematical model for a twin-propeller twin-rudder ship. J. Soc. Nav. Archit. Jpn. 163, 109–118. https://www.jstage.jst.go.jp/article/jjasnaoe1968/1988/163/1988_163_109/_article/.

Ministry of Land, Infrastructure, Transport and Tourism of Japan, 2020. Measured Wave Data of January 2020 on Kobe Port. Nationwide Ocean Wave Information Network for Ports and Harbours. https://nowphas.mlit.go.jp/pastdata_select/2020/1/2020/1/. Accessed : 20 Novermber 2020.

Motora, S., 1959. On the measurement of added mass and added moment of inertia for ship motions. J. Soc. Nav. Archit. Jpn. 105, 83–92 (in Japanese). https://www.jstage.jst.go.jp/article/jjasnaoe1952/1959/105/1959_105_83/_article/-char/en.

Motora, S., 1960a. On the measurement of added mass and added moment of inertia for ship motions (part 2. Added mass for the longitudinal motions). J. Soc. Nav. Archit. Jpn. 106, 59–62 (in Japanese). https://www.jstage.jst.go.jp/article/jjasnaoe1952/1960/106/1960_106_a59/_article/-char/en.

Motora, S., 1960b. On the measurement of added mass and added moment of inertia for ship motions (part 3. Added mass for the transverse motions). J. Soc. Nav. Archit. Jpn. 106, 63–68 (in Japanese). https://www.jstage.jst.go.jp/article/jjasnaoe1952/1960/106/1960_106_a63/_article/-char/en.

Nomoto, K., Taguchi, K., Honda, K., Hirano, S., 1956. On the steering qualities of ships. J. Soc. Nav. Archit. Jpn. 99, 75–82 (in Japanese). https://www.jstage.jst.go.jp/article/jjasnaoe1952/1956/99/1956_99_75/_article/-char/en.

Ogawa, A., Koyama, T., Kijima, K., 1977. MMG Report-I, on the mathematical model of maneuvering motion. Bull. Soc. Nav. Arch. Jpn. 575, 192–198 (in Japanese). https://www.jstage.jst.go.jp/article/zogakusi/575/0/575_KJ00001777750/_article/-char/en.

Okuda, R., Yasukawa, H., Sano, M., Hirata, N., Matsuda, A., 2019. Maneuvering simulation of a twin-propeller ship by an equivalent single-rudder model. In: Proceedings of Japan Society of Naval Architects and Ocean Engineers, vol. 29. Himeji (in Japanese).

Oosterveld, M.W.C., Van Oossanen, P., 1975. Further computer-analyzed data of the Wageningen B-screw series. Int. Shipbuild. Prog. 22, 251–262.

Research Committee on Standardization of Mathematical Model for Ship Maneuvering Predictions, 2012. Committee Report P-29. Japan Society of Naval Architects and Ocean Engineers (in Japanese). https://www.jasnaoe.or.jp/research/dl/report_p-29.pdf.

Research Committee on Improvement of Mathematical Model for Ship Maneuvering Predictions, 2014. Committee Report P-34. Japan Society of Naval Architects and Ocean Engineers (in Japanese). https://www.jasnaoe.or.jp/research/dl/report_p-34.pdf.

Stern, F., Agdrup, K., 2009. Proceedings of the Workshop on Verification and Validation of Ship Maneuvering Simulation Methods SIMMAN 2008. FORCE Technology, Lyngby, Denmark.

Sukas, O.F., Kinaci, O.K., Bal, S., 2019. Theoretical background and application of MANSIM for ship maneuvering simulations. Ocean Eng. 192 https://doi.org/10.1016/j.oceaneng.2019.106239.

Taniguchi, K., Tanibayashi, H., Chiba, N., 1967. Investigation into the propeller cavitation in oblique flow. J. Zosen Kyokai 121, 81–94. https://www.jstage.jst.go.jp/article/jjasnaoe1952/1967/121/1967_121_81/_article/.

Yasukawa, H., Yoshimura, Y., 2015. Introduction of MMG standard method for ship maneuvering predictions. J. Mar. Sci. Technol. 20, 37–52. https://link.springer.com/content/pdf/10.1007%2Fs00773-014-0293-y.pdf.

Yasukawa, H., Hirata, N., Nakayama, Y., 2014. Maneuverability of a semi-displacement typed high speed mono-hull. J. Jpn. Soc. Nav. Archit. Ocean Eng. 19, 47–59 (in Japanese). https://www.jstage.jst.go.jp/article/jjasnaoe/19/0/19_47/_article.

Yoshimura, Y., Nagashima, J., 1985. Estimation of the manoeuvring behavior of ship in uniform wind. J. Soc. Nav. Archit. Jpn. 158, 125–136. https://www.jstage.jst.go.jp/article/jjasnaoe1968/1985/158/1985_158_125/_article/.

Yoshimura, Y., Masumoto, Y., 2011. Maneuvering force database with medium high speed merchant ships including fishing vessels and investigation into a maneuvering prediction method. J. Jpn. Soc. Nav. Archit. Ocean Eng. 14, 63–73 (in Japanese). https://www.jstage.jst.go.jp/article/jjasnaoe/14/0/14_0_63/_article.